BIOCHEMISTRY
including biophysical chemistry & molecular biology

Article

pubs.acs.org/biochemistry

Key Roles of the Downstream Mobile Jaw of *Escherichia coli* RNA Polymerase in Transcription Initiation

Amanda Drennan,[†] Mark Kraemer,[†] Michael Capp,[†] Theodore Gries,[†,#] Emily Ruff,[‡] Carol Sheppard,[§] Sivaramesh Wigneshweraraj,[§] Irina Artsimovitch,[∥] and M. Thomas Record, Jr.*[,†,‡]

[†]Department of Biochemistry, The University of Wisconsin-Madison, Madison, Wisconsin 53706, United States

[‡]Department of Chemistry, The University of Wisconsin-Madison, Madison, Wisconsin 53706, United States

[§]Department of Microbiology and Centre for Molecular Microbiology and Infection, Imperial College London, SW7 2AZ

[∥]Department of Microbiology and Center for RNA Biology, The Ohio State University, Columbus, Ohio 43210, United States

Supporting Information

ABSTRACT: Differences in kinetics of transcription initiation by RNA polymerase (RNAP) at different promoters tailor the pattern of gene expression to cellular needs. After initial binding, large conformational changes occur in promoter DNA and RNAP to form initiation-capable complexes. To understand the mechanism and regulation of transcription initiation, the nature and sequence of these conformational changes must be determined. *Escherichia coli* RNAP uses binding free energy to unwind and separate 13 base pairs of λP_R promoter DNA to form the unstable open intermediate I_2, which rapidly converts to much more stable open complexes (I_3, RP_o). Conversion of I_2 to RP_o involves folding/assembly of several mobile RNAP domains on downstream duplex DNA. Here, we investigate effects of a 42-residue deletion in the mobile β' jaw (ΔJAW) and truncation of promoter DNA beyond +12 (DT+12) on the steps of initiation. We find that in stable ΔJAW open complexes the downstream boundary of hydroxyl radical protection shortens by 5−10 base pairs, as compared to wild-type (WT) complexes. Dissociation kinetics of open complexes formed with ΔJAW RNAP and/or DT+12 DNA resemble those deduced for the structurally uncharacterized intermediate I_3. Overall rate constants (k_a) for promoter binding and DNA opening by ΔJAW RNAP are much smaller than for WT RNAP. Values of k_a for WT RNAP with DT+12 and full-length λP_R are similar, though contributions of binding and isomerization steps differ. Hence, the jaw plays major roles both early and late in RP_o formation, while downstream DNA functions primarily as the assembly platform after DNA opening.

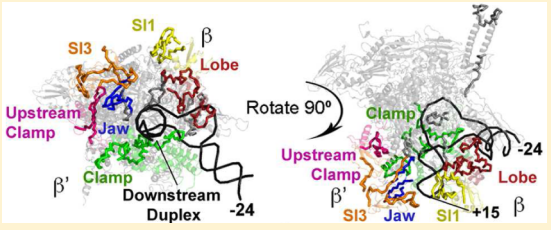

Escherichia coli RNA polymerase (RNAP) is a molecular catalytic machine that synthesizes RNA from a DNA template. Kinetic-mechanistic studies with the WT RNAP and the λP_R promoter as a function of RNAP concentration, upstream DNA length, and solution variables (temperature, salt and solute concentrations), together with footprinting of key intermediates, provide strong evidence that RNAP is also a molecular "isomerization" machine, opening and stabilizing the initiation bubble of promoter DNA in the active site cleft to form a series of open complexes of increasing stability (I_2, I_3, and RP_o; see Figure 1A).[1−4] Early in the mechanism, RNAP bends the upstream ends of both the −35 and −10 regions of the promoter to wrap upstream DNA on the back side of RNAP and to put the downstream duplex in contact with the cleft in the first kinetically significant intermediate I_1.[5,6] Subsequently RNAP actively opens the initiation bubble (−11 to +2) in the cleft to form the initial open complex I_2, in which the start site region of the template strand may be positioned as in RP_o, but the discriminator region of the nontemplate strand is not.[1]

The initial, unstable open complex I_2 is greatly stabilized in the steps converting it to I_3 and RP_o (Figure 1B).[2,3] Analysis of large effects of urea and other solutes on the composite dissociation rate constant k_d reveals that ∼120 amino acid residues fold or are buried in interfaces in the large scale conformational changes that convert I_2 to RP_o, including ∼80 residues in converting I_2 to the subsequent $(I_2{-}I_3)^{\ddagger}$ transition state and ∼40 residues in converting this transition state to RP_o via I_3.[3,7] We proposed that conversion of I_2 to RP_o involves rearrangement of the nontemplate strand in the cleft[1] and assembly of the β' jaw (*E. coli* β' 1150−1208) and other mobile domains of RNAP (called downstream mobile elements, or DMEs; defined in Figure 2A) on downstream duplex DNA.[2,3] Although structural studies of RNAP suggest that the DMEs are rigid bodies, crystallization conditions may select for certain ordered conformations of the DMEs,[7] and PONDR[8] calculations suggest that extensive regions of *E. coli* DMEs are not stably folded in apo-holoenzyme (see Figure 2B and Discussion).[7]

In the present study, we focus on the role of the jaw in the steps of open complex formation at the λP_R promoter. Deletion

Received: September 14, 2012
Revised: October 31, 2012
Published: November 1, 2012

dx.doi.org/10.1021/bi301260u | *Biochemistry* 2012, 51, 9447−9459

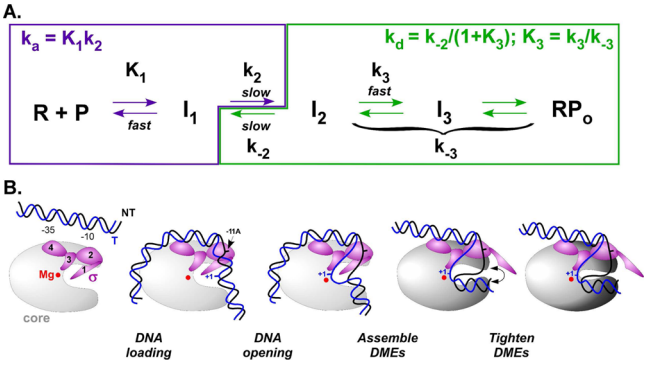

Figure 1. Proposed mechanism of forming and stabilizing the open complex between *E. coli* RNAP and λP_R promoter DNA. (A) Investigation of the kinetics of association of free RNAP (R) with λP_R promoter DNA (P) to form open complexes provides information about the first half of this mechanism, including the equilibrium constant K_1 for binding, bending, and wrapping the DNA duplex to form the advanced closed complex I_1, and the rate constant k_2 for the rate-determining isomerization step (converting I_1 to I_2) in which the DNA duplex is opened in the cleft by RNAP.[1,4,6] Investigation of the dissociation of open complexes provides information about the late steps of the DNA opening mechanism: k_3 is the rate constant for conversion of I_2 to I_3; and k_{-3} is the composite rate constant for conversion of RP_o (or an initial I_3/RP_o mixed population) to I_2. The ratio k_3/k_{-3} is defined as K_3, the equilibrium constant for conversion of I_2 to the equilibrium mixture of I_3 and RP_o.[3] The rate-determining step in dissociation is DNA closing (rate constant k_{-2}). (B) A cartoon model describing the molecular transitions of this mechanism. The active site Mg^{2+} ion is shown as a red ball. The β' mobile jaw is a downstream mobile element (DME) located in the vicinity of the downstream duplex. Here, we propose that the jaw and other DMEs assemble and tighten around the downstream duplex in the late steps of the mechanism to stabilize the late open complexes.

of the jaw (ΔJAW = $\beta'\Delta$1149−1190) is known to reduce the lifetimes of open complexes at several promoters,[9] but its effects on the steps that form and stabilize open complexes have not been previously characterized. The far downstream region of the promoter (+10 to +20), engulfed[10] by interactions with DMEs (Figure 2) in stable open complexes (RP_o), corresponds to the region that has been proposed to interact with the jaw in elongation complexes and heteroduplex promoter complexes.[9,11,12] Importantly, although deletion of the jaw has pleiotropic effects on transcription initiation, elongation, and termination, it does not compromise *E. coli* viability,[9] indicating the lack of gross structural changes in ΔJAW transcription complexes.

Recent studies by James et al. are consistent with a direct interaction between the jaw and the promoter DNA.[13] What is the role of these interactions? Do they participate in promoter opening,[12] or are they responsible for stabilization of the initial unstable open complex (I_2)?[2,3,7] On the basis of comparison of properties of open complexes formed by ΔJAW RNAP and/or a λP_R promoter variant truncated at +12 (DT+12), we conclude that interactions of the jaw, and/or of neighboring DMEs that become repositioned when the jaw is removed, with the far downstream duplex DNA occur primarily in the late conversion of I_3 to RP_o, while interactions of the jaw with in-cleft elements of RNAP, including other DMEs and/or region 1.1 of σ^{70},[14] are responsible for its effects on the early steps of open complex formation.

EXPERIMENTAL PROCEDURES

Buffers. RNAP storage buffer contains 50% glycerol (v/v), 0.01 M Tris (pH 7.5 at 4 °C), 0.1 M NaCl, 0.1 mM DTT, and 0.1 mM Na_2EDTA. Wash buffer for nitrocellulose filter binding experiments contains 0.01 M Tris (pH 8.0 at room temperature), 0.1 M NaCl, and 0.1 mM Na_2EDTA. Phosphate buffer (PB) for dissociation kinetic experiments in the absence of Mg^{2+} is 0.01 M $Na_2HPO_4^-$, 0.16 M NaCl (0.14−0.30 M NaCl in salt dependence experiments), 1 mM dithiothreitol (DTT), and 100 μg/mL BSA. Tris buffer (TB), a common transcription buffer used here for kinetics experiments in the presence of Mg^{2+}, is 0.04 M Tris (adjusted to pH 8.0 at the experimental temperature with HCl), 0.12 M KCl, 0.01 M $MgCl_2$, 1 mM DTT, and 100 μg/mL BSA. Low salt Tris buffer (LSTB) is the same as TB, but with 0.06 M KCl and 0.005 M $MgCl_2$. RNAP storage buffer was added to keep the glycerol concentration constant in a series of association experiments (where the RNAP concentration was varied) and in dissociation experiments (6% total RNAP storage buffer in TB and LSTB; 13% in PB). For MnO_4^- footprinting experiments, DTT was omitted; for HO• footprinting experiments, the Tris concentration was reduced to 0.01 M.

RNAP Preparation. *E. coli* ΔJAW RNAP core was prepared as described previously.[15] *E. coli* WT RNAP core, σ^{70}, and holoenzyme were endogenously expressed and purified from *E. coli* MG1655[16] as described previously.[1] ΔJAW holoenzyme was reconstituted by incubating ΔJAW RNAP core (500 nM) and WT σ^{70} (2 μM) for 90 min at 37 °C.

λP_R Promoter DNA Preparation. Full-length (FL) λP_R DNA duplex fragments (~180 bp long; approximately −120 to +60) were PCR-amplified from plasmid pPR59 (λP_R −59 to +34, a gift from Dr. Wilma Ross)[17] using downstream primer 5′-CAGGACCCGGGGCGCGCTTAATTAACACTCTTA-TACATTATTCC-3′ and upstream primer 5′-GTAC-GAATTCGATATCCAGCTATGACCATGATTACGC-CAGC...3′. Fragments were isolated using the Qiagen QIAquick PCR Purification Kit (Valencia, CA). To end label the template strand downstream, duplex fragments were cleaved with BssHII, and the 5′ phosphates were removed with Antarctic Phosphatase and replaced with [γ-^{32}P] ATP using T4 polynucleotide kinase. The 3′ ends were filled in using Sequenase with 1 mM dGTP + dCTP, and the upstream end was cut with EcoRV to remove the upstream label. For nontemplate strand downstream fill-in label, duplex fragments were cleaved with EcoRV and BssHII, and filled in with [α-^{32}P] dCTP (along with 1 mM cold dGTP + dCTP) using Sequenase.

Downstream-truncated (at +12; DT+12) λP_R DNA duplex fragments (~140 bp long; approximately −120 to +12) were obtained by PCR as above, using the same upstream primer as for full-length λP_R (see above) and downstream primer 5′-GAGGACCCGGGTTACTACATGCAACCATTAT-CACCGCCAGAG-3′. To fill-in label the upstream end of the template strand, the PCR product was cleaved with *Eco*RI and *Sma*I, and labeled with [α-^{32}P] dATP (added with 1 mM cold dATP + dTTP) using Sequenase.

Enzymes used in λP_R promoter DNA preparation and labeling were obtained from New England Biolabs (Ipswitch, MA), except for Sequenase, which was obtained from Affymetrix (Santa Clara, CA). All labeled fragments were purified on a 5% acrylamide gel and isolated using an Elutip-d

dx.doi.org/10.1021/bi301260u | *Biochemistry* 2012, 51, 9447−9459

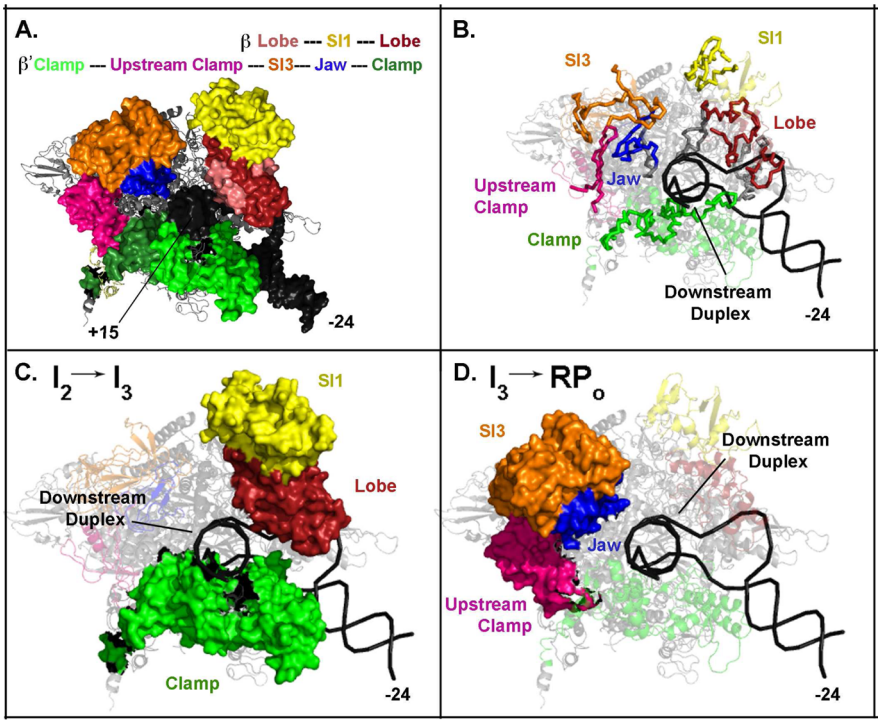

Figure 2. DMEs and their proposed stepwise assembly on downstream DNA to stabilize the initial open complex (I_2) in transcription initiation. (A) DMEs of the β and β' subunits (surface representation) surrounding the downstream DNA duplex (black, to +15) are defined on a model of the *E. coli* RNAP transcription elongation complex.[22] DMEs include the β lobe (red, β 184−224, 344−438); the β sequence insertion (SI)1 (yellow, β 225−343); the β' clamp (green, β' 131−347, 1260−1368); the β' upstream clamp (pink, β' 808−912); β' SI3 (orange, β' 943−1130); and the β' jaw (blue, β' 1149−1208). All residue numbers refer to *E. coli* RNAP. (B) Regions of β and β' in *E. coli* RNAP[22] that are predicted to be unstructured (primarily DMEs) by the PONDR (Predictor of Natural Disordered Regions) VL-XT program are represented by brightly shaded ribbons (see Supporting Information). (C) In the conversion of I_2 to I_3 (or the preceding transition state), a step in which approximately 80 RNAP residues are buried by folding/assembly/binding,[3] we propose that the β' clamp and/or β lobe assemble on the proximal DNA duplex (+3 to +10). (D) In the conversion of I_3 (or the previous transition state; see text) to RP_o, a step in which approximately 40 RNAP residues are buried by folding/assembly/binding,[3] we deduce that the β' jaw and neighboring DMEs assemble on the distal downstream DNA (+10 to +20).

Purification Minicolumn (Whatman (GE Healthcare, Pittsburgh, PA)).

Dissociation Assays. For dissociation kinetic assays, an initial population of 90 ± 10% open complexes was obtained by incubation of excess WT or ΔJAW RNAP holoenzyme (5−20 nM active) with ^{32}P-labeled λP_R promoter (~150 pM) at 25 or 37 °C. Irreversible dissociation was initiated by addition of 50−100 μg/mL heparin, a nondisplacing competitor for both WT[18] and ΔJAW RNAP (Figure S2, Supporting Information). For studies of effects of urea on dissociation, urea was added at the same time as heparin. As a function of time, 100 μL aliquots (~3000 cpm) were removed and applied to nitrocellulose filters on a vacuum manifold.[4] Filters were dried under heat lamps and counted with a Hewlett-Packard Tri-Carb 2100 TR scintillation counter. In TB, about 20% of open complexes formed by ΔJAW RNAP are found to be nondissociating. Addition of urea reduces the initial population of ΔJAW open complexes, making it difficult to quantify the dissociation rate constant k_d accurately as a function of urea in TB. Experiments with WT and ΔJAW RNAP to determine effects of urea on k_d were therefore performed at a convenient NaCl concentration (0.16 M) in PB, the buffer used to determine the effects of univalent salt concentration on k_d.

Analysis of Dissociation Data. Filter-retained counts were corrected by subtracting background counts (determined by filtering solutions in the absence of RNAP) to determine cpm_t, the filter-retained counts due to open complexes. For each data set, the dissociation rate constant k_d was determined by fitting cpm_t vs time to the first order rate equation

$$cpm_t = A + B\exp(-k_d t) \quad (1)$$

where $A = cpm_{t=\infty}$ (which can differ from background because of a subpopulation of nondissociating complexes) and $B = cpm_{t=0} - cpm_{t=\infty}$. The fraction of promoter DNA in the form of open complexes at time t (θ_t) is calculated as $\theta_t = (1/E)(cpm_{t=0}/cpm_{tot})$ where cpm_{tot} is the total cpm in the aliquot filtered and E is the efficiency of retention of open complexes on the nitrocellulose filter membrane, typically in the range 0.6−0.9 (see below) depending on the details of how the filters are prepared and how the filter bound complexes are treated with wash buffer.[3] In Figures 5 and 6, the quantity plotted is $\Delta\theta = \theta_t - \theta_{t=\infty}$, where $\theta_{t=\infty} = (1/E)(cpm_{t=\infty}/cpm_{tot})$. All data fitting, analysis and normalization were performed using Igor Pro Version 5.03.

Determination of the Equilibrium Constant K_3 for Stabilization of the Initial Open Complex by Assembly of Downstream Mobile Elements. Values of K_3 (defined in Figure 1) were determined from experimental values of dissociation rate constants k_d using the relationship[3]

$$K_3 = k_{-2}/k_d - 1 \cong k_{-2}/k_d \text{ for } k_d << k_{-2} \quad (2)$$

The value of the DNA closing rate constant k_{-2} for WT RNAP and FL λP_R promoter DNA at 25 °C was interpolated from results at 10 and 37 °C,[3] using the experimentally determined

dx.doi.org/10.1021/bi301260u | *Biochemistry* 2012, 51, 9447−9459

Table 1. Dissociation Rates of ΔJAW and WT RNAP Open Complexes and Their Interpretation: Effects of [Urea][a]

RNAP	λPR	relative dissociation rate[b]	10^{-3} K_3 (M^{-1})[c]	ΔG_3^{0c} (kcal/mol)	urea dependence of k_d (d ln kd/d[urea]) (M-1)[d]
WT	FL	1	~63	−6.5 ± 0.3	3.1 ± 0.1
WT	DT+12	23 ± 3	~2.7	−4.7 ± 0.3	1.9 ± 0.2
ΔJAW	FL	67 ± 7	~0.9	−4.1 ± 0.3	2.1 ± 0.1
ΔJAW	DT+12	52 ± 11	~1.2	−4.2 ± 0.4	2.1 ± 0.1

[a]Conditions: PB (0.16 M NaCl), 25 °C. [b]Calculated for WT/FL dissociation rate constant $k_d = (2.7 \pm 0.2) \times 10^{-5}$ s^{-1} for these conditions (Figure 5). [c]K_3 and ΔG_3^0 defined as in Figure 1. K_3 is the composite equilibrium constant and ΔG_3^0 is the corresponding standard free energy change for the process of converting the initial open complex I_2 to the equilibrium population of stable open complexes (RP_o, I_3) for λP_R at 25 °C. K_3 calculated from eq 2 using a DNA closing rate constant $k_{-2} = 1.7 \pm 0.4$ s^{-1} at 25 °C, obtained by interpolation of WT/FL results.[3] Uncertainty in K_3 ~ 30−45%. [d]Slopes of plots (Figure 6D) of ln k_d vs [urea].

activation energy (9.9 kcal/mol). This DNA closing rate for WT RNAP and FL λP_R is independent of urea concentration; the entire effect of urea on k_d is on K_3.[3] A preliminary dissection of the dissociation kinetics for ΔJAW RNAP−FL λP_R complexes (E. Ruff, unpublished) indicates that the difference in k_d between ΔJAW and WT RNAP is largely in K_3, and that the effect of urea in both cases is primarily on K_3. We assume that this situation also applies for DT+12 λP_R. For the dissociation of WT RNAP from FL λP_R the uncertainty in k_{-2} is approximately 20%,[3] and that in K_3 is approximately 30%.

Association Assays. To initiate association, excess WT or ΔJAW RNAP (1−50 nM active) was added to ^{32}P-labeled λP_R promoter (~150 pM) in TB at 37 °C. At selected times after mixing, 100 μL aliquots (~3000 counts) were withdrawn. Heparin (50 μg/mL final) was added for 10 s and each aliquot was filtered and counted as described above.

Analysis of Association Data. Association experiments for ΔJAW RNAP at low concentrations (e.g., in Figure 8 in Results) do not go to completion under the conditions investigated, and kinetic data were therefore analyzed as reversible associations[4] according to eq 3:

$$\mathrm{cpm}_t = \mathrm{cpm}_{t=0} + (\mathrm{cpm}_{eq} - \mathrm{cpm}_{t=0})(1 - \exp(-\beta t)) \quad (3)$$

where β is the decay to equilibrium rate constant, cpm_t is the background-corrected counts retained on the filter at time t, and cpm_{eq} and $\mathrm{cpm}_{t=0}$ are the values of cpm_t at equilibrium and extrapolated to $t = 0$, respectively. The decay rate constant β is related to the rate constants k_d and α of dissociation and association, respectively, by

$$\beta = k_d + \alpha = \alpha/\theta_{eq} \quad (4)$$

where θ_{eq} is the fraction of promoter DNA in the form of competitor-resistant (open) complexes at equilibrium, and

$$\alpha = K_1 k_2 [\mathrm{RNAP}]/(1 + K_1[\mathrm{RNAP}]) \quad (5)$$

where K_1 is the equilibrium constant for forming the I_1 intermediate closed complex and k_2 is the isomerization (DNA opening) rate constant.[4] The composite association rate constant k_a (Table 1) is given by[4]

$$k_a = K_1 k_2 \quad (6)$$

If association is irreversible, then $\theta_{eq} = 1$, $k_d = 0$, and $\beta = \alpha$. More generally, determination of α from β requires knowledge of either θ_{eq} or k_d. Determination of θ_{eq} from the experimental quantities cpm_{eq} and cpm_{tot} (the background-corrected total cpm in each filtered aliquot) requires knowledge of the filter efficiency E, the fraction of competitor resistant (open) complexes in solution that are retained on the filter:[4]

$$\mathrm{cpm}_{eq}/\mathrm{cpm}_{tot} = \theta_{eq}^{obs} = E\theta_{eq} \quad (7)$$

Therefore, from eqs 4 and 7,

$$\beta\theta_{eq}^{obs} = E(\beta - k_d) \quad (8)$$

Analysis of the variation in experimental values of $\beta\theta_{eq}^{obs}$ vs β for a series of experiments at different [RNAP] yields best-fit values of E and k_d, allowing calculation of θ_{eq} and α from each determination of β using eq 4. For the sets of experiments analyzed here, efficiencies E of 0.62, 0.77, and 0.81 were obtained for WT-DT+12 complexes, ΔJAW-FL complexes, and ΔJAW-DT+12 complexes, respectively. Values of E and θ_{eq} were used to calculate θ_t for Figure 8. For WT RNAP and DT +12 promoter DNA, values of α obtained from eq 4 were analyzed as a hyperbolic function of [RNAP] using eq 5 to obtain k_a, K_1, and k_2. For ΔJAW RNAP, where α is observed to be proportional to [RNAP] over the accessible concentration range, only k_a is obtained from the analysis. Igor Pro Version 5.03 was used for data fitting and analysis.

$KMnO_4$ Footprinting. Open complexes (5 nM active RNAP + ~1 nM ^{32}P-λP_R promoter DNA) were formed in TB (-DTT) or LSTB (-DTT) by incubation for 30 min at 37 °C. After incubation, heparin (100 μg/mL) was added to some samples for 10 s before addition of $KMnO_4$ to eliminate short-lived complexes. $KMnO_4$ (1.25 mM final concentration) was added for 10 s (determined to be a single-hit dose) and reactions were quenched with 1 M β-mercaptoethanol. Samples were then cleaved with 1 M piperidine, purified, and run on an 8% acrylamide gel together with control (-RNAP) lanes.[19,20]

HO• Footprinting. Open complexes were formed in LSTB at 37 °C as described for $KMnO_4$ footprinting, except that buffers contained DTT and were prepared with a reduced Tris concentration (10 mM) because Tris scavenges HO•.[21] After a brief (10 s) challenge with 100 μg/mL heparin, $[Fe\text{-}EDTA]^{-2}$ (1.8 mM Fe^{2+}, 4.2 mM EDTA) and sodium ascorbate (1.2 mM) were added, followed by addition of H_2O_2 (0.1%) to generate HO•. After 10 s, a short enough exposure time to be in the single-hit regime, reactions were quenched (11.7 mM thiourea + 2.0 μM EDTA) and worked up by phenol extraction and ethanol precipitation. Samples were run on an 8% acrylamide gel.[6,10]

Gel Imaging and Analysis. Footprinting and transcription gels were imaged using either a Typhoon 9410 Variable Mode Imager or a Typhoon FLA-9000 (both from GE Healthcare) and analyzed using Image Quant TL. HO• line scans were normalized to a short region of the footprint upstream of −60. This upstream normalization provides a better match of downstream as well as upstream baselines for the different line scans on each gel than is achieved by normalization to any group of downstream bands or to total cpm. While small drifts

dx.doi.org/10.1021/bi301260u | Biochemistry 2012, 51, 9447−9459

in the downstream baselines are observed with this normalization (visible in the difference line scans in Figure 4E,F), they are not large enough to affect the semiquantitative conclusions of our analysis. To reduce noise, a moving average of 10 positions (approximately 0.7% of the length of the gel) was applied to each line scan (Excel). Difference line scans for each DNA strand were determined by measuring the distance between the free DNA backbone and RNAP-complexed DNA backbone for each DNA base position +1 to +22. For each strand, distances were normalized to the maximum distance, averaged with the independent (duplicate) experiment, and plotted in a bar graph to more explicitly portray the relative protection of WT and ΔJAW RNAP open complexes.

Prediction of RNAP Disordered Regions. The *E. coli* RNAP β and β' subunits[22] were analyzed using VL-XT, the most stringent program in PONDR[8] (Predictions of Naturally Disordered Regions). Only sequences in which at least 15 sequential residues are predicted to be disordered were considered, and predicted disordered sequences known to be in subunit−subunit interfaces were excluded.

RESULTS AND ANALYSIS

$KMnO_4$ Footprints of λP_R Promoter DNA in ΔJAW Complexes. How does the highly conserved bacterial jaw domain affect the distribution and structure of RNAP-promoter complexes? Ederth et al. observed that ΔJAW RNAP forms unstable complexes at the λP_R promoter at 30 °C at moderate salt concentration (0.01 M $MgCl_2$, 0.15 M KCl).[9] To eliminate the possibility that a mixed population of complexes and free promoter DNA exists under these conditions, we sought conditions to increase the stability and lifetime of ΔJAW RNAP complexes at the λP_R promoter (Figure 3A) for footprinting

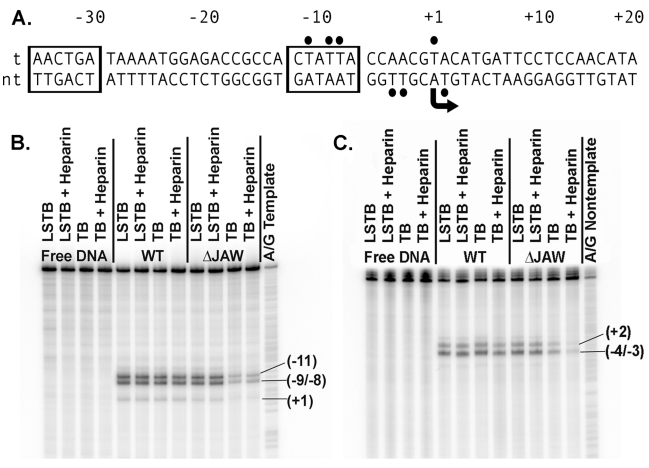

Figure 3. MnO_4^- cleavage of unstacked (single-stranded) thymine residues of λP_R promoter DNA−RNAP open complexes. (A) Sequence of λP_R promoter DNA positions −35 to +20. The −35 and −10 elements of the promoter, which interact with σ regions 4.2 and 2.3/2.4, respectively,[5] are boxed. MnO_4-reactive thymines in WT RNAP open complexes are denoted by bullets above and below the template (t) and nontemplate (nt) strands, respectively. (B, C) Comparison of $KMnO_4$ footprints of λP_R promoter DNA in ΔJAW and WT RNAP open complexes in TB (0.01 M Mg^{2+}, 0.12 M K^+) and in LSTB (0.005 M Mg^{2+}, 0.06 M K^+) at 37 °C: (B) template strand; (C) nontemplate strand. Positions of reactive thymine residues are indicated; nontemplate strand thymines at positions −7 and −10 are not reactive to MnO_4^- because they are protected by interactions with σ.[37]

experiments. At 37 °C in lower-[salt] buffer (LSTB: 0.005 M $MgCl_2$, 0.06 M KCl), ΔJAW RNAP-λP_R open complexes are long-lived (Figure 3B,C; LSTB lanes), suggesting that all bound DNA is in the form of an open complex.

To compare extents of DNA opening, we exposed ΔJAW and WT RNAP complexes to $KMnO_4$ in either LSTB or TB (0.01 M $MgCl_2$, 0.12 M KCl). $KMnO_4$ preferentially oxidizes unstacked thymines, providing a method of detecting and quantifying DNA opening in RNAP-promoter complexes.[1,20,23] We find that ΔJAW-λP_R complexes are open: thymines at −11, −9, −8 and +1 on the template strand (Figure 3B) and −4, −3 and +2 (but not −7 and −10) on the nontemplate strand (Figure 3C)) exhibit the same $KMnO_4$ reactivity, and therefore are exposed to the same extents in the open regions of WT-λP_R and ΔJAW-λP_R open complexes. In TB, detected thymines on both strands in ΔJAW open complexes are significantly less $KMnO_4$-reactive than in WT open complexes (Figure 3B,C; TB lanes). Though ΔJAW open complexes are less stable and shorter-lived in TB than in LSTB, this cannot explain the large reductions in $KMnO_4$ reactivity (see below). For both WT and ΔJAW RNAP, λP_R promoter DNA opening and closing rate constants are only weakly (if at all) dependent on salt concentration[3] (E. Ruff, unpublished), so this is not a salt effect on DNA opening. Nor can it be a salt effect on $KMnO_4$ reactivity, since the $KMnO_4$ reactivities of these thymines in WT open complexes are the same in TB as in LSTB.

HO• Footprints of λP_R Promoter DNA in ΔJAW Open Complexes. The jaw domain is located near the downstream DNA (Figure 2A), and can interact with DNA nonspecifically.[13,24,25] Furthermore, a large β' region that includes the jaw cross-links to the DNA backbone.[26] However, direct evidence demonstrating jaw contacts to DNA in *any* RNAP−DNA complex (e.g., closed, open, initiation, or elongation states) is lacking. Here, we ask whether the jaw deletion alters protection of the DNA backbone in open promoter complexes. Figure 4 compares normalized line scans from quantitative single-hit HO• footprints of both template (panels A and C) and nontemplate (panels B and D) strands of FL λP_R in stable open complexes formed by either WT or ΔJAW RNAP in LSTB at 37 °C. (Sequencing gels for the experiments in panels A and B are shown in Figure S1, Supporting Information.) Bar graphs of average differences in HO• protection between open complexes and free promoter DNA at each downstream position from +1 to +22 are shown in Figure 4E,F.

Two very significant differences are observed in HO• footprints of ΔJAW and WT open complexes. First, the downstream boundaries of HO• protection of both strands in the ΔJAW RNAP open complex are shorter than for WT RNAP. The boundary on the template strand (Figure 4E) is approximately 1 helical turn shorter for the ΔJAW open complex than for that formed by WT RNAP, ending near +10 instead of +20. For the nontemplate strand (Figure 4F), the downstream boundary of the ΔJAW RNAP open complex is near +15, about 0.5 helical turn shorter than that observed for WT RNAP (+20). (The difficulty in quantitatively normalizing the entire length of these >100 nucleotide line scans is revealed in the drift in the region downstream of the boundary of the WT footprint at +20, observed in the difference plots in Figure 4E,F. This drift is not large enough to affect the semiquantitative results presented above, though it does increase the uncertainty in assignment of the downstream boundary of the ΔJAW footprints (sequence position +10 ± 2 bases on the template strand and position +15 ± 3 bases on the nontemplate

dx.doi.org/10.1021/bi301260u | *Biochemistry* 2012, 51, 9447−9459

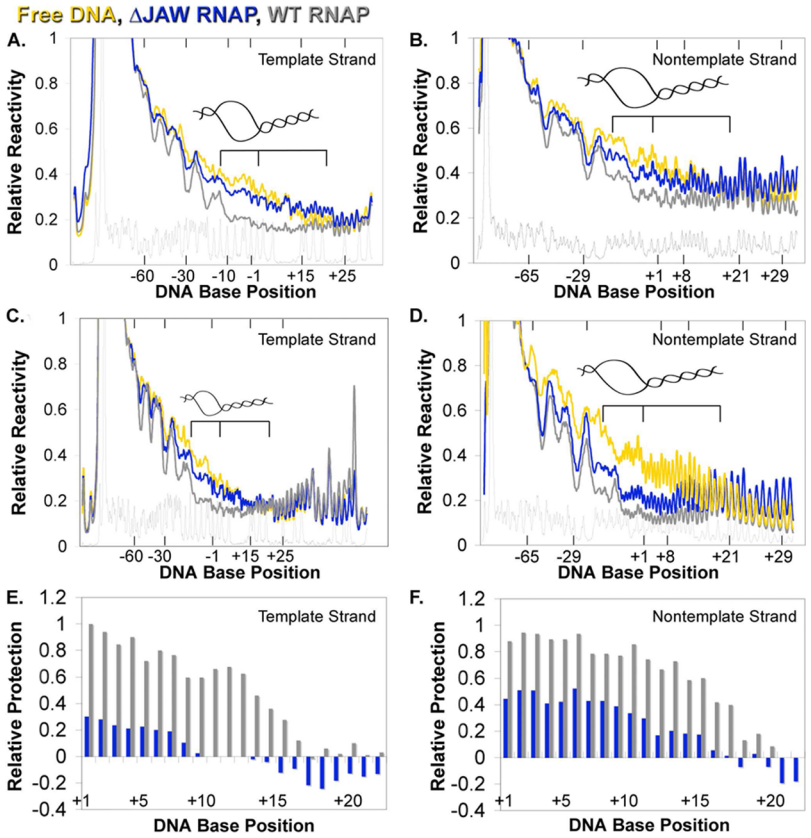

Figure 4. Line scans of lanes in single-hit HO• footprinting experiments (Figure S1) performed in duplicate for the template (A,C) and nontemplate (B, D) strands of λP_R promoter DNA in open complexes with ΔJAW RNAP (blue) or WT RNAP (gray) and free λP_R DNA (gold) in LSTB at 37 °C. The regions of the DNA initiation bubble (−11 to +2) and the downstream DNA duplex (+3 to +20) are indicated by brackets below a model of these DNA regions. Bar graphs in panels E and F display the relative protection of individual downstream positions of template (E) and nontemplate (F) strands in ΔJAW and WT open complexes, calculated as the average of difference line scans for each strand (see Experimental Procedures). Each panel is normalized so the maximum difference in protection in this interval is set equal to 1.0.

strand).) The reduction in HO• protection of the ΔJAW RNAP open complex provides direct evidence that the jaw, and/or neighboring regions of RNAP perturbed by deleting the jaw, likely contacts one side of the duplex DNA from +10 to +20 in WT RP_o. Direct contact between the jaw and the distal downstream duplex (+10 to +20) was proposed previously.[9,24,26] However, structural studies of bacterial RNAP suggested that the interaction between the jaw and the DNA downstream duplex is proximal to the transcription start site, forming an interface only to about +12.[22,25] In this case, the presence of the jaw might act indirectly by influencing the concurrent folding/assembly of one or more additional DMEs onto the distal downstream duplex. At this time, we are not able to distinguish between these two possibilities.

A second very striking difference between HO• footprints of ΔJAW and WT open complexes, shown for the downstream region of the promoter DNA analyzed in Figure 4E,F (but also clearly observable in the upstream promoter regions in Figure 4A−D), is that all regions of both DNA strands in the ΔJAW open complex are significantly less protected from HO• than is the case for WT RP_o. This effect extends at least from −45 to the downstream boundary of the footprint and is especially pronounced in the open region of the promoter (initiation bubble; −11 to +2) in the active site cleft. This global reduction in protection cannot be attributed simply to the shorter lifetime of the ΔJAW open complex, which is more than 1 h in LSTB and therefore much longer than the time scale of the footprinting experiments (10 s). In TB, the ΔJAW open complex exhibits no significant HO• protection of either template or nontemplate strand (data not shown), even though the lifetime of the ΔJAW complex in TB (30 min) is much greater than the time required to footprint (10 s; see below), and $KMnO_4$ footprints (Figure 2) reveal that this complex is an open complex.

A plausible explanation of the reduced protection observed for the ΔJAW RNAP open complex in both buffers is that more water remains in the ΔJAW RNAP−promoter interface than in the WT RNAP−promoter interface, and that HO• gains access to the DNA in the interface by facilitated diffusion on a network of residual water of hydration. Alternatively, or in addition, the ΔJAW RNAP−promoter interface may be more dynamic than that of the WT enzyme, exhibiting normal modes of vibration that result in local separations of RNAP and promoter DNA that allow HO• access to all portions of the interface in a 10 s footprinting experiment without any global dissociation.

Large Effects of Deletion of the Jaw or of Downstream Promoter DNA on the Rate of Dissociation of Open Complexes. To investigate when, where, and how strongly the jaw and neighboring DMEs assemble on the downstream duplex in the process of forming the stable open complex at λP_R, we compared the kinetics of dissociation of open complexes formed by WT and ΔJAW RNAP on FL and truncated (at +12) λP_R promoter DNA (DT+12). Dissociation

dx.doi.org/10.1021/bi301260u | *Biochemistry* 2012, 51, 9447−9459

time courses in PB (0.16 M NaCl) at 25 °C are shown in Figure 5A. Dissociation rate constants k_d calculated from these

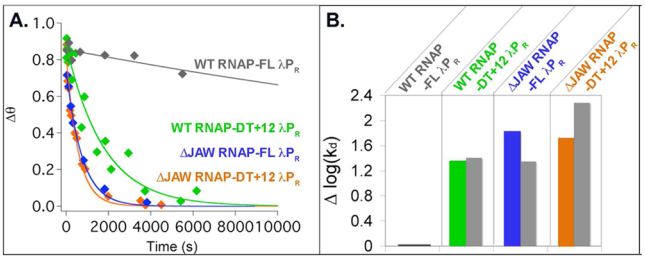

Figure 5. Kinetics of dissociation of WT and variant open complexes in PB (0.16 M Na^+) at 25 °C (panel A), as compared to results in TB (0.01 M Mg^{2+}, 0.12 M K^+) at 37 °C (panel B). (A) Fraction of dissociable open complexes remaining at time t ($\Delta\theta$; see Experimental Procedures), determined using the nitrocellulose filter assay in PB with excess heparin as competitor (Table 1). Complexes investigated include WT RNAP at FL (gray) or DT+12 (green) λP_R promoter DNA and ΔJAW RNAP at FL (blue) and DT+12 (orange) λP_R promoter DNA. (B) Relative dissociation rate constants of variant complexes expressed relative to WT-FL complexes. Results in PB (green, blue, and orange bars, as determined by studies shown in panel A) are compared with those in TB (gray bars, as determined by the nitrocellulose dissociation assay (WT complexes) or decay to equilibrium data (ΔJAW complexes; see Table 2)).

data (see Table 1) are compared with one another, and with the corresponding quantities determined at 37 °C in TB (0.12 M KCl, 0.01 Mg^{2+}), in Figure 5B. Values of k_d in TB, obtained by analysis of reversible association kinetic experiments (shown in Figure 8 below) are listed in Table 2. In both PB (25 °C) and TB (at 37 °C), WT-FL open complexes are long-lived. Dissociation rate constants k_d for WT-FL open complexes are small and of comparable magnitude ($k_d = 2.7 \times 10^{-5}$ s^{-1} in PB at 25 °C; $k_d = 2.2 \times 10^{-5}$ s^{-1} in TB at 37 °C[18]), permitting convenient study of the destabilizing effects of urea on k_d of the less stable variant complexes.

For both sets of solution conditions, effects of deletion of the jaw or of the downstream DNA on k_d are large (~20–60-fold increase in k_d from that observed for dissociation of WT RNAP from FL λP_R). Details differ somewhat in the two conditions investigated. In TB, each single variant increases k_d approximately 25-fold; in PB, deleting the jaw increases k_d even more dramatically (67-fold), while the effect of deleting the downstream duplex is similar to that observed in TB. The additional effect of the second deletion (comparing k_d for ΔJAW-DT+12 with k_d for ΔJAW-FL or WT-DT+12) is small in PB at 25 °C, but larger in TB at 37 °C. In PB at 25 °C, deletion of the downstream DNA in ΔJAW open complexes does not affect the dissociation rate, and deletion of the jaw in open complexes formed with DT+12 DNA increases the dissociation rate by only a small amount (~2-fold) compared to WT RNAP. In TB at 37 °C, however, deletion of the downstream DNA in ΔJAW open complexes increases the dissociation rate by approximately 8-fold. These differences between the variants in PB and TB probably result from specific effects of Mg^{2+}; previous dissociation studies with WT RNAP and FL λP_R as a function of Mg^{2+} concentration provided evidence for binding of 2–3 Mg^{2+} ions in the conversion of I_2 to RP_o.[27]

Because $k_d = k_{-2}/(1 + K_3)$, where k_{-2} is the DNA closing rate constant (the bottleneck step in dissociation) and K_3 is the composite equilibrium constant for forming the stable open complex (RP_o, I_3, or an equilibrium mixture of the two) from I_2 (Figure 1), these large effects on k_d of deleting either the jaw or the downstream DNA could result from a combination of increases in k_{-2} and/or reductions in K_3. For WT RNAP, the large effect of urea on k_d arises from K_3, while k_{-2} is independent of urea concentration.[3] Because deletion of either the jaw or the downstream duplex significantly reduces the urea dependence of k_d (as shown in Figure 6D below), we infer that the primary effect of these deletions must be on K_3. Consistent with this deduction, preliminary measurements of k_{-2} for dissociation of ΔJAW RNAP from FL λP_R promoter DNA (E. Ruff, unpublished) reveal that it is similar to (indeed somewhat smaller than) k_{-2} for WT RNAP.

Values of the equilibrium constant K_3 and the standard free energy change ΔG_3^0 for conversion of I_2 to the stable open complex obtained from these data using eq 2 are listed in Tables 1 and 2 for the two conditions investigated. For WT RNAP and FL λP_R, the full stabilization of the open complex is ~ −7 kcal/mol (K_3 of order 10^5), as determined previously.[3] A similar conclusion was obtained from dissociation kinetic studies with DT heteroduplexes.[12] Tables 1 and 2 show that deletion of either the far downstream duplex (at +12) or of the jaw eliminates approximately one-third of the stabilization provided by the DME assembly. In PB, deletion of *both* the downstream duplex (at +12) and the jaw has no additional effect, as expected if the main effect of deleting the jaw is to eliminate interactions of DMEs with region +12 to +20 of the

Table 2. Rate and Equilibrium Constants for the Steps of Transcription Initiation at the λP_R Promoter at 37 °C[a]

RNAP	λP_R	relative dissociation rate[b]	10^{-3} K_3 (M^{-1})[c]	ΔG_3^{0c} (kcal/mol)	10^{-6} k_a[d] (M^{-1} s^{-1})	10^{-6} K_1[d] (M^{-1})	k_2 (s^{-1})[d]
WT	FL	1	~150	−6.7 ± 0.3	3.8 ± 0.7[e]	6.6 ± 2.7[e]	0.66 ± 0.27[e]
	DT+12	25 ± 3	~5.9	−5.4 ± 0.3	5 ± 2	40 ± 20	0.14 ± 0.09
ΔJAW	FL	23 ± 3	~6.6	−5.5 ± 0.3	0.33 ± 0.05[f]	nd[g]	nd[g]
	DT+12	180 ± 80	~0.8	−4.2 ± 0.8	0.33 ± 0.05[f]	nd[g]	nd[g]
WT	UT-47[h]	0.9 ± 0.3	~170	−7.4 ± 0.5	0.5 ± 0.1	26 ± 2	0.02 ± 0.003

[a]Conditions: TB (0.01 M $MgCl_2$, 0.12 M KCl), 37 °C. [b]Calculated for WT/FL dissociation rate constant $k_d = 2.2$ (±0.3) $\times 10^{-5}$ s^{-1} for these conditions.[18] Values of k_d for variants were determined from reversible association kinetic data of Figure 8 using eq 8 (see Experimental Procedures). [c]K_3 and ΔG_3^0 are defined in Figure 1 and Table 1 footnote *c*; at 37 °C for λP_R, these quantities presumably refer to the process of converting I_2 to RP_o. K_3 is calculated from eq 2 using a DNA closing rate constant $k_{-2} = 3.3$ (±0.7) s^{-1} at 37 °C.[3] Uncertainty in K_3 is ~30% except for ΔJAW-DT +12 and WT-UT-47 where it is ~75% and ~60%, respectively. [d]Values of k_a, K_1, and k_2 obtained from eqs 5 and 6; k_a is the composite second-order association rate constant for open complex formation, K_1 is the composite equilibrium constant for forming the I_1 closed complex, and k_2 is the isomerization rate constant for converting closed intermediate I_1 to open intermediate I_2. [e]Ref 4. [f]Association results for ΔJAW RNAP at FL and DT +12 λP_R promoters were fit together. [g]Not able to be determined from these data. [h]Dissociation and association rate constants for WT RNAP at upstream-truncated (at −47; UT-47) λP_R.[19]

dx.doi.org/10.1021/bi301260u | *Biochemistry* 2012, 51, 9447–9459

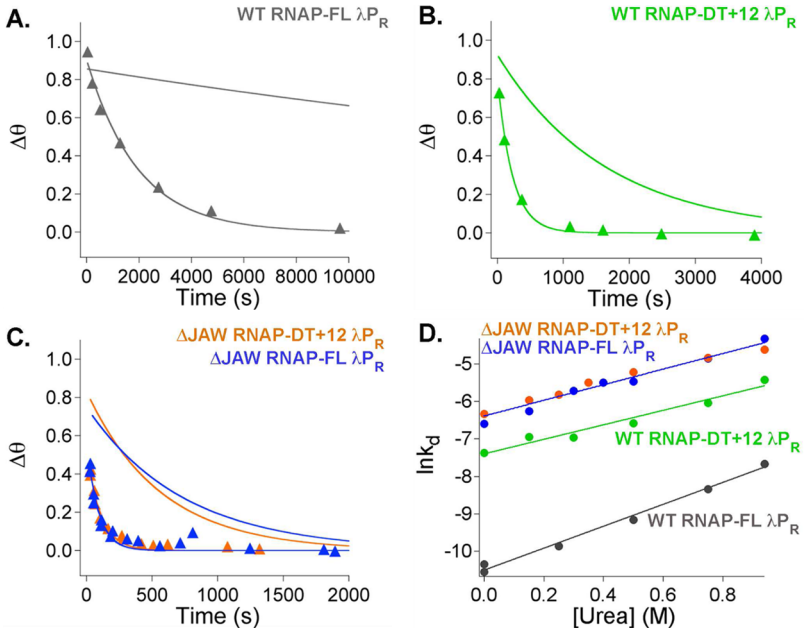

Figure 6. Effects of urea on the dissociation rate constant k_d, used as a probe of coupled folding and assembly of DMEs (Figure 2), including the jaw, on downstream DNA. Experiments were performed using the nitrocellulose filter assay in PB at 25 °C. Panels A–C compare dissociation time courses in 0.94 M urea (triangles), plotted as in Figure 5A, with those in the absence of urea (fits reproduced from Figure 5A). (A) WT-FL λP_R (gray). (B) WT-DT+12 λP_R (green). (C) ΔJAW-FL (blue) or -DT+12 λP_R (orange). (D) Plot of ln k_d vs urea molarity, comparing dissociation of WT and ΔJAW RNAP from FL and DT+12 λP_R promoter DNA. Colors are coded to panels A–C. The fitted line for the combined ΔJAW-FL and ΔJAW-DT+12 data set is blue. Slopes (d ln k_d/d[urea]) are listed in Table 1.

downstream duplex. Effects observed in both buffers indicate that removal of the jaw disrupts a salt- and Mg^{2+}-dependent network of contacts of DMEs with each other and with the distal downstream duplex, greatly reducing K_3 and the lifetime of the open complex and greatly increasing its HO• reactivity.

Effects of Urea on Dissociation Rate Constants k_d for WT vs Variant Open Complexes. The effect of urea on dissociation rate constants for WT RNAP-FL λP_R open complexes in PB is as large as that observed for unfolding a small globular protein (100–150 residues),[28] which we interpreted in terms of the folding and assembly of DMEs on the downstream duplex DNA (+3 to +20) in the process of converting I_2 to RP_o.[3,7] If deletion of the jaw and/or the downstream duplex reduces the folding and assembly of DME on the downstream DNA in these late steps, then dissociation of these variant open complexes should exhibit a smaller dependence on urea concentration than for the WT-FL RP_o. Panels A–C of Figure 6 compare the kinetics of dissociation of WT-FL and variant open complexes in 0.94 M urea with that observed in the absence of urea (from Figure 5A). These panels illustrate the general observation that the effect of urea on the rate of dissociation of WT-FL RP_o is much larger than the effect of urea on the rates of dissociation of the ΔJAW RNAP and DT +12 downstream deletion variants. Dissociation rate constants k_d obtained from these data and analogous experiments at intermediate urea concentrations are plotted on a log scale (ln k_d) vs urea concentration for these four situations in Figure 6D. Linear fits represent the data well in all cases, with intercepts (compared with WT RNAP-FL λP_R in Table 1) that agree within uncertainty with the experimentally determined dissociation rate constants in the absence of urea (Figure 5A).

Slopes obtained from linear fits (d ln k_d/d[urea]) are listed in Table 1. For dissociation of WT-FL RP_o in PB, d ln k_d/d[urea] = 3.1 M^{-1}, the same within uncertainty as that reported previously in TB at 17 °C (3.0 M^{-1}).[7] For the three single and double variant open complexes formed with ΔJAW RNAP and/or DT+12 λP_R, d ln k_d/d[urea] is only 2/3 as large (d ln k_d/d[urea] = 1.9–2.1 M^{-1}). From eq 2, these urea derivatives of k_d are equal in magnitude and opposite in sign to the corresponding urea derivatives of K_3, because the DNA closing rate constants k_{-2} are independent of urea concentration for WT[3] and ΔJAW (E, Ruff, unpublished) RNAP. Deletion of the jaw, of the downstream duplex at +12, or of both, eliminates one-third of this urea effect.

Dissection of urea effects on the dissociation rate constant k_d for WT RNAP-FL λP_R open complexes reveals that two-thirds of it is in conversion of I_2 to the $(I_2 - I_3)^{\ddagger}$ transition state, with the other one-third in the conversion of this transition state to I_3 and then to RP_o.[3] Both the urea results and the reductions in open complex lifetime observed for the jaw deletion and/or downstream DNA truncation indicate that by these criteria the ΔJAW-FL λP_R final open complex is more similar to $(I_2 - I_3)^{\ddagger}$ or I_3 than to RP_o. Comparison of the effects of urea on dissociation of open complexes formed by WT and ΔJAW RNAP at FL and DT+12 λP_R with these kinetic-mechanistic results argues strongly that the jaw assembles with other DMEs on the downstream duplex promoter DNA late in the mechanism of RP_o formation, most likely in the conversion of I_3 to RP_o, and that the final open complex formed by ΔJAW RNAP is a plausible model of the intermediate I_3 formed by WT RNAP at FL λP_R. Relative dissociation rate constants (Tables 1 and 2) are consistent with this conclusion, as are the different effects of salt concentration on dissociation rate constants of WT and ΔJAW open complexes, presented next.

Effects of Salt Concentration on Dissociation Kinetics of the ΔJAW RNAP–FL λP_R Open Complex are Consistent with an I_3-like Open Complex. Figure 7 compares the effects of NaCl concentration on dissociation

dx.doi.org/10.1021/bi301260u | Biochemistry 2012, 51, 9447–9459

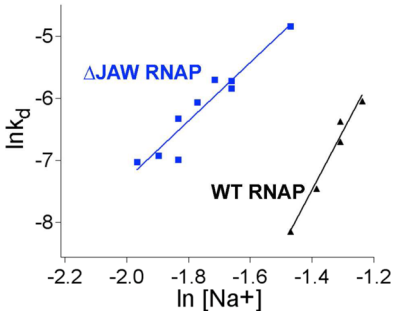

Figure 7. Comparison of effects of [Na^+] on dissociation rate constants k_d of open complexes formed by ΔJAW (blue squares) and WT RNAP (black triangles)[2] at FL λP_R in PB, 25 °C. Slopes of these plots (d ln k_d/d ln[Na^+]) are listed in Table 3.

rate constants for WT-FL open complexes at 25 °C[2] and ΔJAW-FL open complexes at 25 °C in PB. Paralleling the reduced effect of urea on k_d for ΔJAW open complex dissociation (33% reduction compared to WT RNAP), dissociation of the ΔJAW open complex in PB is much less salt concentration dependent (50% reduction in d ln k_d/d ln[Na^+]; see Table 3) than dissociation of RP_o formed by WT

Table 3. Salt Effects on Dissociation Kinetics of ΔJAW and WT RNAP Open Complexes[a]

RNAP	λP_R	relative dissociation rate[b]	10^{-3} K_3 (M^{-1})[b,c]	ΔG_3^0 (kcal/mol)[d]	d ln k_d/ d ln[Na^+][e]
WT	FL	1	6.0 ± 1.0	−5.2 ± 0.3	9.5 ± 1.0
ΔJAW	FL	28 ± 3	0.21 ± 0.05	−3.2 ± 0.2	4.7 ± 0.7

[a]Conditions: PB, 25 °C. [b]At 0.23 M Na^+ where, for WT RNAP, k_d = (2.8 ± 0.1) × 10^{-4} s^{-1}, interpolated from Figure 7. [c]Calculated using k_{-2} = 1.7 ± 0.4 s^{-1} at 25 °C, interpolated from results at 10 and 37 °C.[3] [d]Calculated from K_3. [e]Determined from Figure 7.

RNAP at FL λP_R. While the previous kinetic data for WT RNAP did not allow the salt effect on k_d to be uniquely dissected into contributions from the individual steps of dissociation, as was done for the urea effect,[3] the greatly reduced salt effect on dissociation of the ΔJAW open complex is completely consistent with the proposal that this complex is I_3-like, with a salt dependence which is halfway between that of RP_o (d ln k_d/d ln[Na^+] = 9) and that of the initial open complex I_2 (d ln k_d/d ln[Na^+] = 0).

Early Steps of ΔJAW–λP_R Open Complex Formation. We previously proposed that DMEs have large effects on early as well as late steps of open complex formation.[5,6] Here, we use association kinetic studies to test our hypothesis that the jaw participates in the steps leading up to and/or including opening ($R + P \rightleftarrows I_1 \rightarrow I_2$; Figure 1). For a series of concentrations of ΔJAW RNAP, all in excess over promoter DNA, time courses of open complex formation at FL and DT+12 λP_R at 37 °C in TB are plotted in Figure 8A,C. Analogous results for association of WT RNAP at DT+12 λP_R are plotted in Figure 8B. In all cases the kinetics are single-exponential, demonstrating that the initial binding step(s) ($R + P \rightleftarrows I_1$) are in rapid equilibrium on the time scale of the subsequent slow step ($I_1 \rightarrow I_2$) involving DNA opening.[29]

At all but the highest RNAP concentrations investigated, the kinetics of association of ΔJAW RNAP with both FL and DT +12 (Figure 8A,C) are reversible, forming equilibrium mixtures of open complexes and unbound promoter DNA. By contrast, time courses of association of WT RNAP with FL λP_R[4] and with DT+12 λP_R (Figure 8B) are irreversible. Values of RNAP-concentration-dependent composite association rate constants α (eq 5) for ΔJAW RNAP at FL and DT+12 λP_R, obtained as described in Experimental Procedures from the decay-to-equilibrium data in Figure 8A,C, are plotted vs concentration of ΔJAW RNAP in Figure 8D. Also plotted in Figure 8D are values of α for the association of WT RNAP with DT+12 λP_R (Figure 8B), and fitted curves summarizing the RNAP-concentration-dependences of α previously reported for association of WT RNAP with FL λP_R[4] and with upstream-truncated (UT-47) λP_R.[19]

From Figure 8D, rates of open complex formation from free reactants at all but the lowest RNAP concentrations are slower for all variants than for the WT-FL case. In particular, values of the rate constant α for the ΔJAW variant and either FL or DT +12 λP_R are as small as those observed previously for association of WT RNAP with UT-47 λP_R.[19] Removing either the jaw or the upstream DNA reduces the rate of open complex formation to a similarly large extent. This finding supports our previous proposal that the upstream clamp, jaw, and other DMEs function as a relay system, in which the upstream clamp interacts with the far upstream DNA in the wrapped I_1 intermediate, and this interaction shifts the positions of the jaw and other DMEs to open a gate in the downstream cleft and allow entry of the downstream duplex prior to opening.[5,6] Removing only the downstream DNA (i.e., open complex formation by WT RNAP with DT+12 λP_R) reduces α to a much smaller though still significant extent at higher RNAP concentrations.

Initial slopes of plots of α vs RNAP concentration (Figure 8D) are overall second-order rate constant for open complex formation k_a (eq 6). Values of k_a for WT RNAP and either FL or DT+12 λP_R are similar, and are approximately 10-fold larger than those for ΔJAW RNAP and either FL or DT+12 λP_R, or for WT RNAP and UT-47 λP_R. This large effect on k_a of deleting the jaw cannot be explained entirely by an interaction of RNAP with the downstream duplex in I_1 or the subsequent transition state, since the same behavior is observed with both FL and DT+12 λP_R. This is consistent with the deduction from the k_d data that the jaw deletion has large effects on the interaction of DMEs with the downstream duplex late in RP_o formation, in the conversion of I_3 to RP_o.

From eq 6, k_a is the product of the equilibrium constant K_1 for formation of the I_1 closed complex and the rate constant k_2 for the isomerization step, including DNA opening, that converts I_1 to I_2. For situations where K_1 and the range of RNAP concentrations investigated are large enough, individual values of K_1 and k_2 are obtained from analysis of the dependence of α on [RNAP] using eq 5. For open complex formation by WT RNAP, truncation of the downstream duplex (DT+12), like upstream truncation (UT-47), increases K_1 and reduces k_2. For DT+12, these effects compensate, so the overall k_a is unaffected by downstream truncation; for UT-47, Davis et al. found that the reduction in k_2 was the dominant effect, greatly reducing k_a even though K_1 increased.[19] For open complex formation by ΔJAW RNAP with either FL or DT+12 λP_R, the data do not permit dissection of k_a into K_1 and k_2.

The finding that association rate constants k_a are the same for open complex formation by ΔJAW RNAP and FL or DT+12 λP_R promoter (Table 2) appears to contradict what is observed in Figure 8, where decay to equilibrium rates at a specified [RNAP] are faster for ΔJAW-DT+12 complexes (Figure 8C)

dx.doi.org/10.1021/bi301260u | Biochemistry 2012, 51, 9447−9459

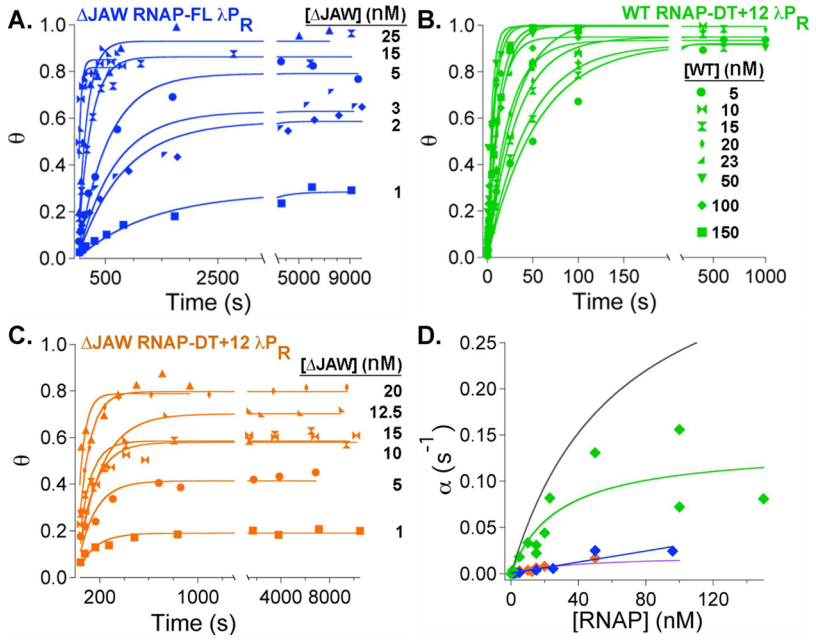

Figure 8. Comparison of association kinetics of ΔJAW and WT RNAP with FL and DT+12 λP_R promoter DNA in TB at 37 °C. Panels A–C display time courses of the fraction of λP_R promoter DNA in the form of heparin-resistant open complexes (θ) for different RNAP concentrations for (A) ΔJAW RNAP and FL λP_R promoter (blue), (B) WT RNAP and DT+12 λP_R promoter (green), and (C) ΔJAW RNAP and DT+12 λP_R promoter (orange). Curves are single exponential fits to eq 3, yielding decay to equilibrium rate constants β, from which the association rate constant α is obtained (eq 4). (D) Plots of α vs [RNAP] for the data of panels A–C, compared with published fits for association of WT RNAP with FL (gray)[4] and UT-47 λP_R (purple).[19] The axes of the inset figure are the same as in the main panel. A hyperbolic fit (eq 5) to the WT-DT+12 data set (green curve) and a linear fit to the combined ΔJAW-FL and ΔJAW-DT+12 data set (blue line) are shown. Values obtained from these fits are reported in Table 2.

than for ΔJAW-FL complexes (Figure 8A). This is not a contradiction; the faster decay to equilibrium is entirely because k_d for dissociation of ΔJAW-DT+12 open complexes is larger than for ΔJAW-FL open complexes in TB (Table 2).

DISCUSSION

In fundamental and significant ways, the mechanism of forming and stabilizing the open RNAP-λP_R promoter complex resembles the mechanism of an enzyme-catalyzed reaction.[1,5] First, in a series of steps that are rapidly reversible, like those that form a precatalytic complex between enzyme and substrates, RNAP binds the start-site region of duplex promoter DNA, bends it, and inserts it into the active site cleft.[3,6,19] Then, in a slow (rate-determining) step occurring in the active site cleft, like the catalytic step of an enzyme-catalyzed reaction, RNAP opens the initiation bubble (−11 to +2) and appears to place the +1 template strand base in the active site.[1] Subsequent to opening, the downstream half of the melted nontemplate strand appears to be repositioned, and RNAP DMEs assemble and fold on the distal downstream duplex.[1−3,7] For the conditions used to investigate dissociation of open complexes here, the steps of DME disassembly are rapidly reversible on the time scale of the rate determining DNA closing step. For both enzyme catalyzed reactions and transcription initiation, the early and late reversible steps are the targets of most regulatory factors and ligands.

In this study, we probed the role of RNAP interactions with the downstream DNA by removing either the DNA downstream beyond +12 or the jaw, which is thought to interact with the downstream DNA. Footprinting reveals that ΔJAW open complexes differ structurally from those formed by the WT RNAP: although the DNA is melted to the same extent, both DNA strands are globally less protected from HO• attack, and the downstream boundary of HO• protection shortens by 5–10 bp. Dissociation kinetics of ΔJAW open complexes are faster and less dependent on urea concentration, whereas promoter binding-DNA opening is much slower than for WT RNAP. These results implicate the jaw role during both early and late steps in RP_o formation. By contrast, the downstream DNA appears to function primarily after DNA opening: while DT+12 truncation has the same effect on dissociation kinetics as the removal of the jaw, it does not affect association rate constant k_a for WT RNAP.

Consistent with the reported effects of the jaw deletion on the lifetime of the open complex,[9,14] we deduce that the jaw is required for RNAP contacts with the distal downstream region (+10 to +20) of the promoter established in the last step of stabilization of the open complex (conversion of I_3 to RP_o). Strikingly, however, we also find that deletion of the jaw greatly reduces the rate of the early steps of initiation. We deduce that this effect is not simply due to loss of interactions with the downstream DNA; a loss of interactions of the jaw with in-cleft elements such as other DMEs and/or with region 1.1 of σ^{70} must also be involved.[14] This interpretation is consistent with observations of Mekler et al. that gp2, a phage inhibitor that binds to the jaw, destabilizes RNAP/scaffold complexes even in the absence of downstream DNA.[24] In addition, results of HO• footprinting suggest that the jaw is required to seal the downstream end of the cleft in RP_o, eliminating water and forming a tight interface of RNAP-DNA backbone interactions that is highly protected from HO• attack. By contrast, the open DNA strands and surrounding duplex in the I_3-like ΔJAW open complex appear to be more hydrated, as judged by their increased HO• reactivity. Expulsion of water during RP_o

dx.doi.org/10.1021/bi301260u | *Biochemistry* 2012, 51, 9447−9459

formation presumably contributes significantly to the entropic driving force for the endothermic steps of opening and conversion of the initial open complex (I_2) to RP_o, as previously proposed.[2]

Our current and previous results indicate that assembly of DMEs on the downstream duplex stabilizes the initial open complex I_2 in converting it to RP_o.[2,3] Analysis of RNAP binding to heteroduplex downstream junction templates with progressively shortened downstream DNA duplex revealed that many interactions contribute to this stabilizing effect.[12] The largest incremental effect was observed when the duplex was extended from +8 to +9. Structural studies suggest that DNA near +9 contacts the jaw directly.[25] This interaction likely plays a role in formation and stabilization of RP_o and is subject to control by gp2[13] and likely other regulators.

However, structural analysis of RNAP shows that the jaw does not extend beyond +10, raising a question of how the far downstream protection is established. Collectively, the available data suggest that contacts between the jaw and promoter DNA set the trajectory for DNA entry into a trough formed by the jaw and clamp domains. Single-molecule FRET experiments demonstrate that the clamp is open in free RNAP but closes upon the formation of RP_o.[30] While the open state of the clamp permits DNA movement in and out of the cleft, interactions of DNA with RNAP trigger an inward 16° rotation of the clamp, effectively sealing the cleft in RP_o. The observed protection from HO• is likely due to a combination of the cleft closure and direct contacts between DMEs and DNA.

Cross-linking data support the existence of direct interactions between DNA backbone from +10 to +20 and a large fragment of the β' subunit (residues 821−1407), which includes the clamp, the jaw, and SI3.[26] Given the range of motions demonstrated[30] and proposed[22] for these DMEs, we cannot pinpoint specific interactions of RNAP regions with each position in the promoter DNA. Furthermore, DMEs are proposed to function together in several relay systems (Figure 2),[5,13] and changes in different elements may give rise to similar effects on transcription, e.g., in the case of the jaw and SI3, which share an extensive interface.[31] Thus, it is difficult to distinguish between direct (mediated via DNA contacts) and indirect effects of deletions in individual DMEs. A more refined mapping of the DME contacts with the promoter DNA awaits high-resolution structural and cross-linking analysis of RP_o.

We propose that in ΔJAW RNAP-promoter complexes, the downstream DNA may not be properly positioned in the trough, and clamp closure is subsequently inhibited. The same effect is observed upon addition of gp2, which blocks DNA interactions with the jaw[30] and locks the clamp in the open state.[13]

The Role of the Jaw in Early (Pre-Opening) Steps. The profound effects of deleting the jaw on the early steps of open complex formation, observed for both FL and DT+12 promoter DNA, indicate that the jaw and/or neighboring regions affected by its deletion are a key part of the proposed relay system[5,6] by which the upstream promoter sequence, transcription factors, ligands and solution variables work together to regulate the rate of forming the initial open complex (I_2), and thereby regulate the rate of transcription initiation. The limited evidence available to date suggests that much of this regulation occurs in the steps that put the downstream DNA duplex in the cleft. The subsequent opening step is relatively independent of solute concentration[2,7] suggesting that, like catalytic steps of enzymes, it occurs within a somewhat sealed cleft that is not readily accessible to solutes and regulatory ligands.

We have proposed that these early acting upstream regulatory factors have a common basis of action: together they set or modify the trajectory of far-upstream DNA in early, relatively unstable closed intermediate complexes (designated RP_c) in which the promoter DNA lies outside the cleft.[5] The trajectory of far-upstream DNA determines its ability to interact with the upstream clamp, which in turn affects the positioning of the jaw and other DMEs.[6] More specifically, we proposed that when −35 and UP elements are recognized by σ^{70} region 4 and the αCTDs (respectively), far-upstream DNA is bent and wrapped around the back of RNAP, in close proximity to the downstream end of the active site cleft and the upstream clamp. These interactions trigger release of DMEs from their blocking positions, opening the downstream gate to allow entry of the downstream duplex.

Interestingly, yeast RNAP II may also use a molecular relay to mediate loading of the duplex DNA into the active site cleft, which is obstructed in the free enzyme in all multisubunit RNAPs. The Pol II subunit Rpb4/7 (absent in bacterial RNAP) binds to the RNAP core, facilitating clamp closure.[32] Recent studies postulate that subsequent binding of the multisubunit mediator complex attracts Rpb4/7, resulting in formation of the open clamp state and thus allowing for the entry of duplex DNA into the RNAP active site cleft.[33]

The Role of the Jaw in Late (Post-Opening) Steps. The observed dissociation rate constant k_d of stable open complexes (mainly RP_o) to free promoter and RNAP provides information about the steps that convert RP_o back to I_2 and the rate of DNA closing ($I_2 \rightarrow I_1$) (Figure 1). The DNA closing rate (k_{-2}) is not a function of salt or urea concentration.[3] Therefore, solute and salt effects on k_d arise from their effect on the equilibrium constant for conversion of I_2 to RP_o (K_3). For the conditions of our experiments, steps by which RP_o converts to I_2 rapidly equilibrate on the time scale of DNA closing ($I_2 \rightarrow I_1$).[29] We proposed that the conversion of I_2 to RP_o involves assembly of DMEs on the downstream duplex, and movement of the downstream portion of the nontemplate strand in the cleft.[1−3] Our current studies test these proposals by deleting the jaw and/or the downstream duplex (DT+12).

Kontur et al. concluded from the urea effect on k_d that approximately 100−150 residues of RNAP are buried by folding/assembly in the steps converting the initial open complex I_2 to the final open complex RP_o (Figure 2).[3] Roughly two-thirds of this urea effect occurs in the conversion of I_2 to the subsequent $(I_2-I_3)^{\ddagger}$ transition state, and the remaining 40 residues are buried in the conversion of this transition state to RP_o. In the current study, we find that, in contrast to WT enzyme, the ΔJAW variant does not protect the distal downstream DNA from HO• attack. The effect of urea on dissociation of ΔJAW RNAP from either FL or DT+12 λP_R and of WT from DT+12 λP_R indicates that ∼40 fewer residues are buried in the open complex formed by these variants. PONDR predicts that 33 residues near the jaw are unstructured in RNAP (Figure 2B). The simplest explanation of these observations is that the jaw folds and assembles with other DMEs on the distal promoter DNA in the final step of open complex formation (Figure 2D), and that the open complex formed by ΔJAW may therefore be a stable mimic of the relatively unstable I_3 intermediate open complex formed by WT RNAP on the path to RP_o at λP_R.

dx.doi.org/10.1021/bi301260u | Biochemistry 2012, 51, 9447−9459

What events (involving burial of approximately 80 residues by folding/assembly) occur in the conversion of I_2 to I_3? We propose that folding and assembly of regions of the β' clamp and/or the β lobe, DMEs proposed to interact with the proximal downstream DNA duplex (+3 to +9),[9] occur in this step (Figure 2C). PONDR predicts that 99 residues of the β' clamp and 57 residues of the β lobe are unstructured in RNAP. Formation of the proximal downstream contacts would logically precede assembly of the jaw and/or other DMEs to the distal downstream duplex, as stability increases in the conversion of I_2 to RP_o. Experiments are in progress to test these predictions for interactions of the DMEs with downstream DNA in I_2 and I_3, and to determine the effect of promoter sequence and interactions in the cleft on the extent of assembly and tightening of the jaw and other DMEs.

Our studies reveal the existence of three types of "open" promoter complexes that differ in interactions between the downstream duplex DNA with DMEs. We hypothesize that the distribution among these complexes differs at different cellular promoters, underlying their regulation by transcription factors such as DksA, which allosterically alters RNAP contacts with DNA downstream from the active site.[34] We propose that this mode of regulation may be utilized by eukaryotic RNAPs, which have structural elements that are homologous (β' clamp, β lobe) or functionally analogous (β' jaw) to bacterial DMEs.[35] Furthermore, similar to our footprinting results obtained at λP_R, recent single-molecule studies of yeast RNAP II open complexes revealed very different positions of the downstream DNA,[36] supporting our idea that promoter DNA/RNAP interactions in this region are highly dynamic and suggesting that they may contribute to regulation of eukaryotic gene expression.

■ ASSOCIATED CONTENT

Supporting Information

PONDR predictions of naturally disordered regions of the DMEs. Figure S1: Representative HO• footprinting gels; Figure S2: Dissociation of ΔJAW-FL and WT-DT+12 open complexes are not heparin-dependent. This material is available free of charge via the Internet at http://pubs.acs.org.

■ AUTHOR INFORMATION

Corresponding Author

*Tel.: (608) 262-5332; fax: (608) 262-3453; e-mail: mtrecord@wisc.edu.

Present Address

[#]Department of Chemistry, Beloit College, 700 College St., Beloit, WI 53511.

Funding

This work was supported by NIH Grants GM023467 and GM047022 to M.T.R., NSF Grant MCB-0949569 to I.A., grants from the BBSRC and Wellcome Trust to S.W., and by UW-Madison. S.W. is a recipient of a BBSRC David Phillips Fellowship (BB/E023703).

Notes

The authors declare no competing financial interest.

■ ACKNOWLEDGMENTS

We gratefully acknowledge numerous contributions of Dr. Ruth Saecker to the design of this research and comments on the manuscript. We also thank Dr. Wilma Ross for extensive and very helpful comments on an earlier draft of this manuscript. Finally, we thank the reviewers and editor for their careful reading of the manuscript, comments, and constructive criticism.

■ ABBREVIATIONS USED

RNAP, RNA polymerase; WT, wild-type RNAP; DME, downstream mobile element; ΔJAW, deletion of the RNAP jaw ($\Delta\beta'$ 1149−1190); SI, sequence insertion; FL, full-length λP_R promoter DNA; DT+12, truncation of λP_R promoter DNA downstream at +12; UT-47, truncation of λP_R promoter DNA upstream at −47; TB, Tris buffer; LSTB, low salt Tris buffer; PB, phosphate buffer

■ REFERENCES

(1) Gries, T. J., Kontur, W. S., Capp, M. W., Saecker, R. M., and Record, M. T., Jr. (2010) One-step DNA melting in the RNA polymerase cleft opens the initiation bubble to form an unstable open complex. *Proc. Natl. Acad. Sci. U. S. A. 107*, 10418−10423.

(2) Kontur, W. S., Capp, M. W., Gries, T. J., Saecker, R. M., and Record, M. T., Jr. (2010) Probing DNA binding, DNA opening, and assembly of a downstream clamp/jaw in *Escherichia coli* RNA polymerase-λP_R promoter complexes using salt and the physiological anion glutamate. *Biochemistry 49*, 4361−4373.

(3) Kontur, W. S., Saecker, R. M., Capp, M. W., and Record, M. T., Jr. (2008) Late steps in the formation of *E. coli* RNA polymerase-λP_R promoter open complexes: Characterization of conformational changes by rapid [perturbant] upshift experiments. *J. Mol. Biol. 376*, 1034−1047.

(4) Saecker, R. M., Tsodikov, O. V., McQuade, K. L., Schlax, P. E., Jr, Capp, M. W., and Record, M. T., Jr. (2002) Kinetic studies and structural models of the association of *E. coli* σ^{70} RNA polymerase with the λP_R promoter: Large scale conformational changes in forming the kinetically significant intermediates. *J. Mol. Biol. 319*, 649−671.

(5) Saecker, R. M., Record, M. T., Jr, and Dehaseth, P. L. (2011) Mechanism of bacterial transcription initiation: RNA polymerase - promoter binding, isomerization to initiation-competent open complexes, and initiation of RNA synthesis. *J. Mol. Biol. 412*, 754−771.

(6) Davis, C. A., Bingman, C. A., Landick, R., Record, M. T., Jr, and Saecker, R. M. (2007) Real-time footprinting of DNA in the first kinetically significant intermediate in open complex formation by *Escherichia coli* RNA polymerase. *Proc. Natl. Acad. Sci. U. S. A. 104*, 7833−7838.

(7) Kontur, W. S., Saecker, R. M., Davis, C. A., Capp, M. W., and Record, M. T., Jr. (2006) Solute probes of conformational changes in open complex (RP_o) formation by *Escherichia coli* RNA polymerase at the λP_R promoter: Evidence for unmasking of the active site in the isomerization step and for large-scale coupled folding in the subsequent conversion to RP_o. *Biochemistry 45*, 2161−2177.

(8) Romero, P., Obradovic, Z., Li, X., Garner, E. C., Brown, C. J., and Dunker, A. K. (2001) Sequence complexity of disordered protein. *Proteins 42*, 38−48.

(9) Ederth, J., Artsimovitch, I., Isaksson, L. A., and Landick, R. (2002) The downstream DNA jaw of bacterial RNA polymerase facilitates both transcriptional initiation and pausing. *J. Biol. Chem. 277*, 37456−37463.

(10) Craig, M. L., Suh, W. C., and Record, M. T., Jr. (1995) HO• and DNase I probing of $E\sigma^{70}$ RNA polymerase–λP_R promoter open complexes: Mg^{2+} binding and its structural consequences at the transcription start site. *Biochemistry 34*, 15624−15632.

(11) Korzheva, N., Mustaev, A., Kozlov, M., Malhotra, A., Nikiforov, V., Goldfarb, A., and Darst, S. A. (2000) A structural model of transcription elongation. *Science 289*, 619−625.

(12) Mekler, V., Minakhin, L., and Severinov, K. (2011) A critical role of downstream RNA polymerase-promoter interactions in the formation of initiation complex. *J. Biol. Chem. 286*, 22600−22608.

(13) James, E., Liu, M., Sheppard, C., Mekler, V., Camara, B., Liu, B., Simpson, P., Cota, E., Severinov, K., Matthews, S., and

Wigneshweraraj, S. (2012) Structural and mechanistic basis for the inhibition of *Escherichia coli* RNA polymerase by T7 Gp2. *Mol. Cell 47*, 755−766.
(14) Wigneshweraraj, S. R., Burrows, P. C., Severinov, K., and Buck, M. (2005) Stable DNA opening within open promoter complexes is mediated by the RNA polymerase *β′*-jaw domain. *J. Biol. Chem. 280*, 36176−36184.
(15) Camara, B., Liu, M., Reynolds, J., Shadrin, A., Liu, B., Kwok, K., Simpson, P., Weinzierl, R., Severinov, K., Cota, E., Matthews, S., and Wigneshweraraj, S. R. (2010) T7 phage protein Gp2 inhibits the *Escherichia coli* RNA polymerase by antagonizing stable DNA strand separation near the transcription start site. *Proc. Natl. Acad. Sci. U. S. A. 107*, 2247−2252.
(16) Burgess, R. R., and Jendrisak, J. J. (1975) A procedure for the rapid, large-scall purification of *Escherichia coli* DNA-dependent RNA polymerase involving polymin P precipitation and DNA-cellulose chromatography. *Biochemistry 14*, 4634−4638.
(17) Mangiarotti, L., Cellai, S., Ross, W., Bustamante, C., and Rivetti, C. (2009) Sequence-dependent upstream DNA-RNA polymerase interactions in the open complex with λP_R and λP_{RM} promoters and implications for the mechanism of promoter interference. *J. Mol. Biol. 385*, 748−760.
(18) Roe, J. H., Burgess, R. R., and Record, M. T., Jr. (1984) Kinetics and mechanism of the interaction of *Escherichia coli* RNA polymerase with the λP_R promoter. *J. Mol. Biol. 176*, 495−522.
(19) Davis, C. A., Capp, M. W., Record, M. T., Jr, and Saecker, R. M. (2005) The effects of upstream DNA on open complex formation by *Escherichia coli* RNA polymerase. *Proc. Natl. Acad. Sci. U. S. A. 102*, 285−290.
(20) Craig, M. L., Tsodikov, O. V., McQuade, K. L., Schlax, P. E., Jr, Capp, M. W., Saecker, R. M., and Record, M. T., Jr. (1998) DNA footprints of the two kinetically significant intermediates in formation of an RNA polymerase-promoter open complex: Evidence that interactions with start site and downstream DNA induce sequential conformational changes in polymerase and DNA. *J. Mol. Biol. 283*, 741−756.
(21) Tullius, T. D., Dombroski, B. A., Churchill, M. E., and Kam, L. (1987) Hydroxyl radical footprinting: A high-resolution method for mapping protein-DNA contacts. *Methods Enzymol. 155*, 537−558.
(22) Opalka, N., Brown, J., Lane, W. J., Twist, K. A., Landick, R., Asturias, F. J., and Darst, S. A. (2010) Complete structural model of *Escherichia coli* RNA polymerase from a hybrid approach. *PLoS Biol. 8*, e1000483.
(23) Sasse-Dwight, S., and Gralla, J. D. (1989) $KMnO_4$ as a probe for lac promoter DNA melting and mechanism in vivo. *J. Biol. Chem. 264*, 8074−8081.
(24) Mekler, V., Minakhin, L., Sheppard, C., Wigneshweraraj, S., and Severinov, K. (2011) Molecular mechanism of transcription inhibition by phage T7 gp2 protein. *J. Mol. Biol. 413*, 1016−1027.
(25) Vassylyev, D. G., Vassylyeva, M. N., Perederina, A., Tahirov, T. H., and Artsimovitch, I. (2007) Structural basis for transcription elongation by bacterial RNA polymerase. *Nature 448*, 157−162.
(26) Naryshkin, N., Revyakin, A., Kim, Y., Mekler, V., and Ebright, R. H. (2000) Structural organization of the RNA polymerase-promoter open complex. *Cell 101*, 601−611.
(27) Suh, W. C., Leirmo, S., and Record, M. T., Jr. (1992) Roles of Mg^{2+} in the mechanism of formation and dissociation of open complexes between *Escherichia coli* RNA polymerase and the λP_R promoter: Kinetic evidence for a second open complex requiring Mg^2. *Biochemistry 31*, 7815−7825.
(28) Hong, J., Capp, M. W., Saecker, R. M., and Record, M. T., Jr. (2005) Use of urea and glycine betaine to quantify coupled folding and probe the burial of DNA phosphates in lac repressor-lac operator binding. *Biochemistry 44*, 16896−16911.
(29) Tsodikov, O. V., and Record, M. T., Jr. (1999) General method of analysis of kinetic equations for multistep reversible mechanisms in the single-exponential regime: Application to kinetics of open complex formation between $E\sigma^{70}$ RNA polymerase and λP_R promoter DNA. *Biophys. J. 76*, 1320−1329.
(30) Chakraborty, A., Wang, D., Ebright, Y. W., Korlann, Y., Kortkhonjia, E., Kim, T., Chowdhury, S., Wigneshweraraj, S., Irschik, H., Jansen, R., Nixon, B. T., Knight, J., Weiss, S., and Ebright, R. H. (2012) Opening and closing of the bacterial RNA polymerase clamp. *Science 337*, 591−595.
(31) Conrad, T. M., Frazier, M., Joyce, A. R., Cho, B. K., Knight, E. M., Lewis, N. E., Landick, R., and Palsson, B. O. (2010) RNA polymerase mutants found through adaptive evolution reprogram *Escherichia coli* for optimal growth in minimal media. *Proc. Natl. Acad. Sci. U. S. A. 107*, 20500−20505.
(32) Armache, K. J., Kettenberger, H., and Cramer, P. (2003) Architecture of initiation-competent 12-subunit RNA polymerase II. *Proc. Natl. Acad. Sci. U. S. A. 100*, 6964−6968.
(33) Cai, G., Imasaki, T., Yamada, K., Cardelli, F., Takagi, Y., and Asturias, F. J. (2010) Mediator head module structure and functional interactions. *Nat. Struct. Mol. Biol. 17*, 273−279.
(34) Rutherford, S. T., Villers, C. L., Lee, J. H., Ross, W., and Gourse, R. L. (2009) Allosteric control of *Escherichia coli* rRNA promoter complexes by DksA. *Genes Dev. 23*, 236−248.
(35) Werner, F., and Grohmann, D. (2011) Evolution of multi-subunit RNA polymerases in the three domains of life. *Nat. Rev. Microbiol. 9*, 85−98.
(36) Treutlein, B., Muschielok, A., Andrecka, J., Jawhari, A., Buchen, C., Kostrewa, D., Hog, F., Cramer, P., and Michaelis, J. (2012) Dynamic architecture of a minimal RNA polymerase II open promoter complex. *Mol. Cell 46*, 136−146.
(37) Feklistov, A., and Darst, S. A. (2011) Structural basis for promoter-10 element recognition by the bacterial RNA polymerase *σ* subunit. *Cell 147*, 1257−1269.